Supplement of Clim. Past, 12, 213–240, 2016
http://www.clim-past.net/12/213/2016/
doi:10.5194/cp-12-213-2016-supplement

Climate of the Past
Open Access
EGU

Supplement of

Variability in climate and productivity during the Paleocene–Eocene Thermal Maximum in the western Tethys (Forada section)

L. Giusberti et al.

Correspondence to: L. Giusberti (luca.giusberti@unipd.it)

Fig. S1

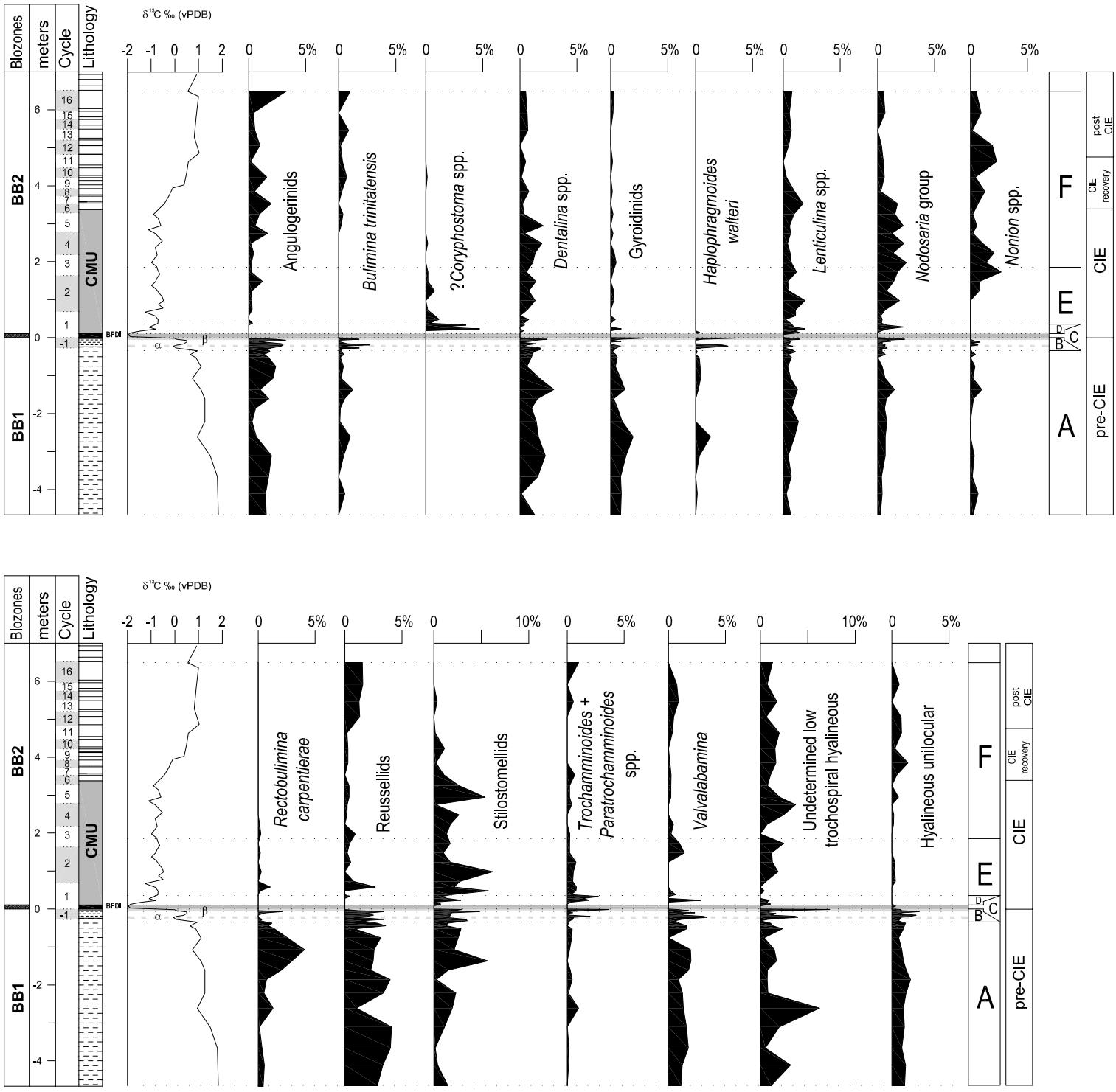

Relative abundance of selected benthic foraminifera (< 5 %) across the PETM at Forada plotted against biostratigraphy, precessional cycles, lithology, δ13C bulk record, recognized benthic foraminiferal assemblages (A to F) and isotopic intervals. Benthic foraminiferal 5 biozonation after Berggren and Miller (1989). The gray bands indicate intervals of carbonate dissolution. α = pre-CIE dissolution, β = burndown layer, BFDI=benthic foraminiferal dissolution interval.

Fig. S2

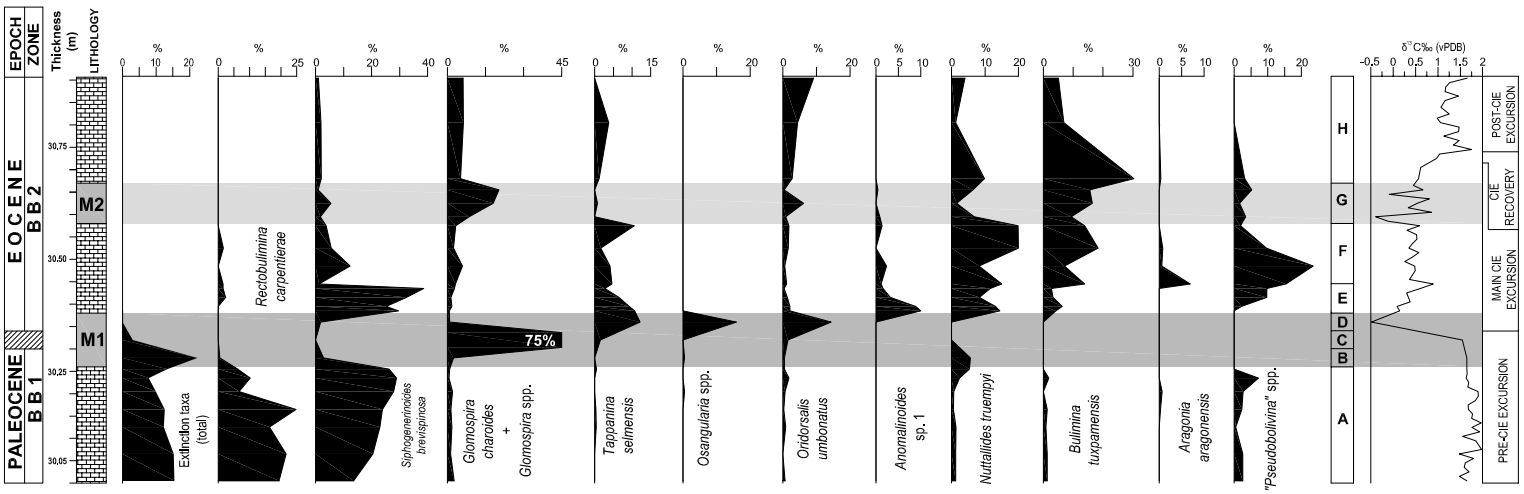

Relative abundance of selected benthic foraminifera across the Paleocene/Eocene boundary at Contessa Road (central Italy) plotted against biostratigraphy, lithology, recognized assemblages (A to H) and δ13C record together with the isotopic intervals. Modified from Giusberti et al. (2009). The gray bands indicate intervals of carbonate dissolution.

Fig. S3

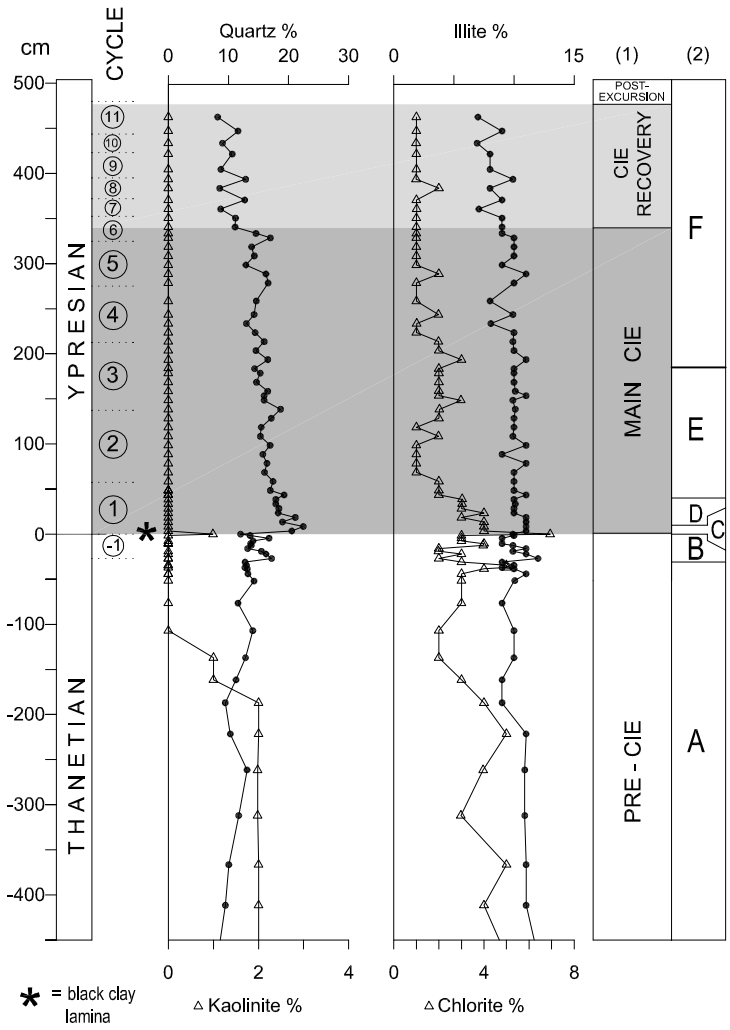

Clay mineral assemblage and quartz % in the upper Paleocene and basal Eocene of the Forada section. (1) Isotopic intervals; (2) Benthic foraminiferal assemblages. Redrawn from Giusberti et al. (2007).

Table S1. Census data of benthic foraminifera across the Paleocene/Eocene boundary in the Forada section (>63 <500 µm size fraction).

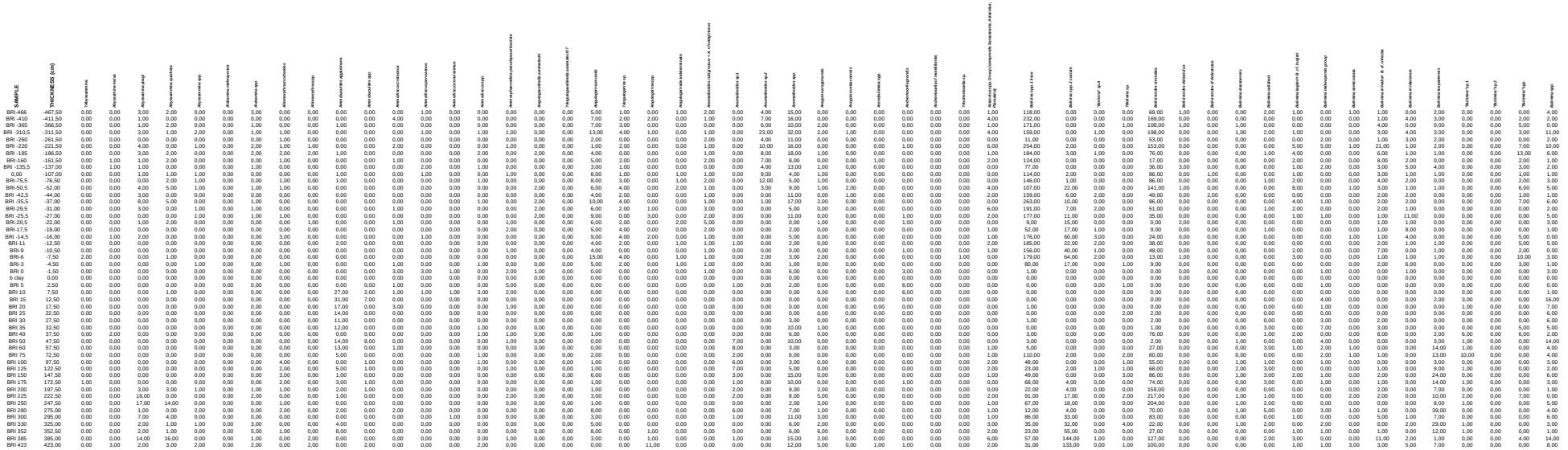

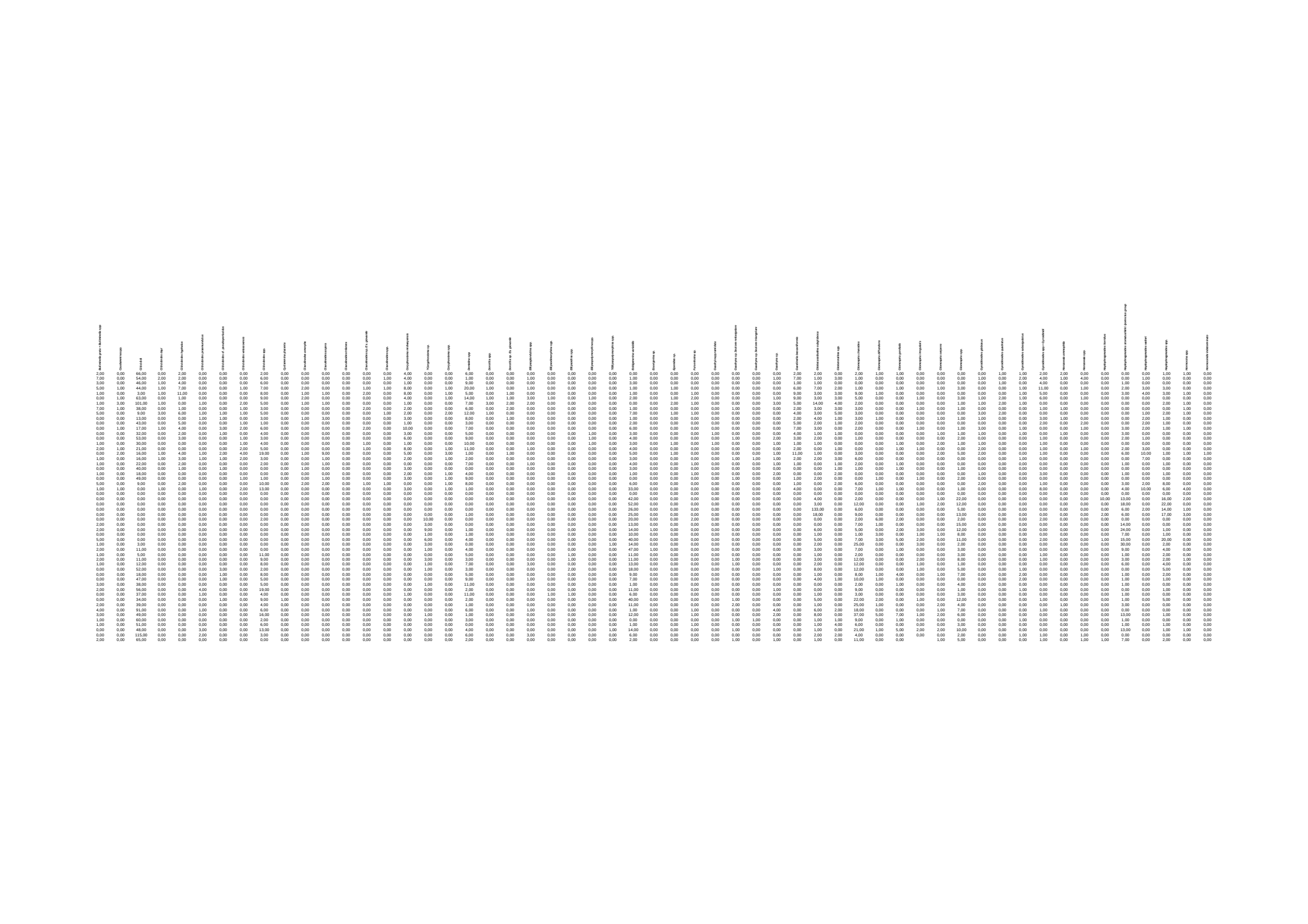

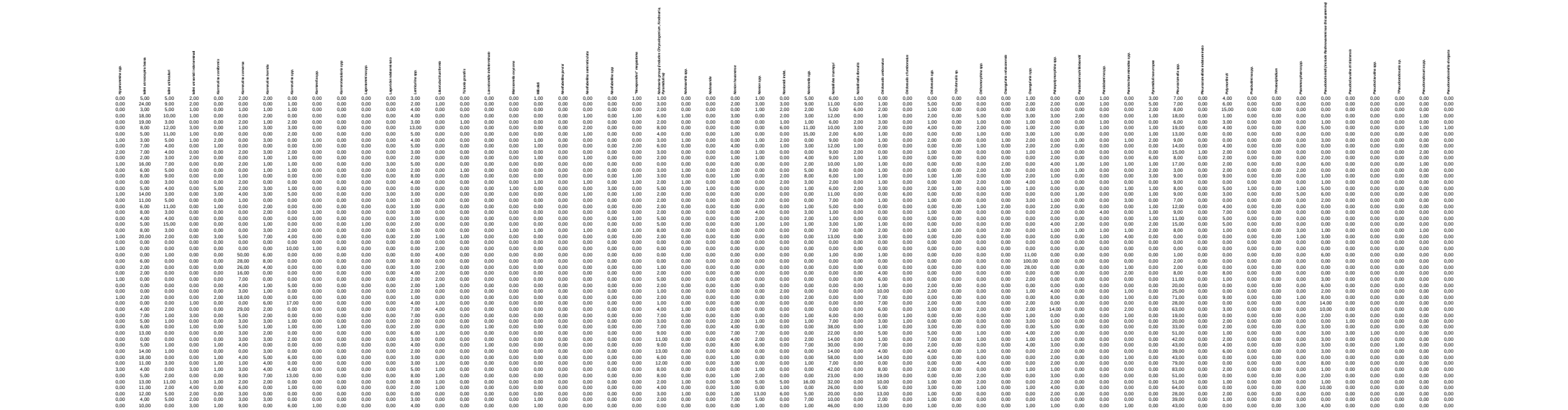

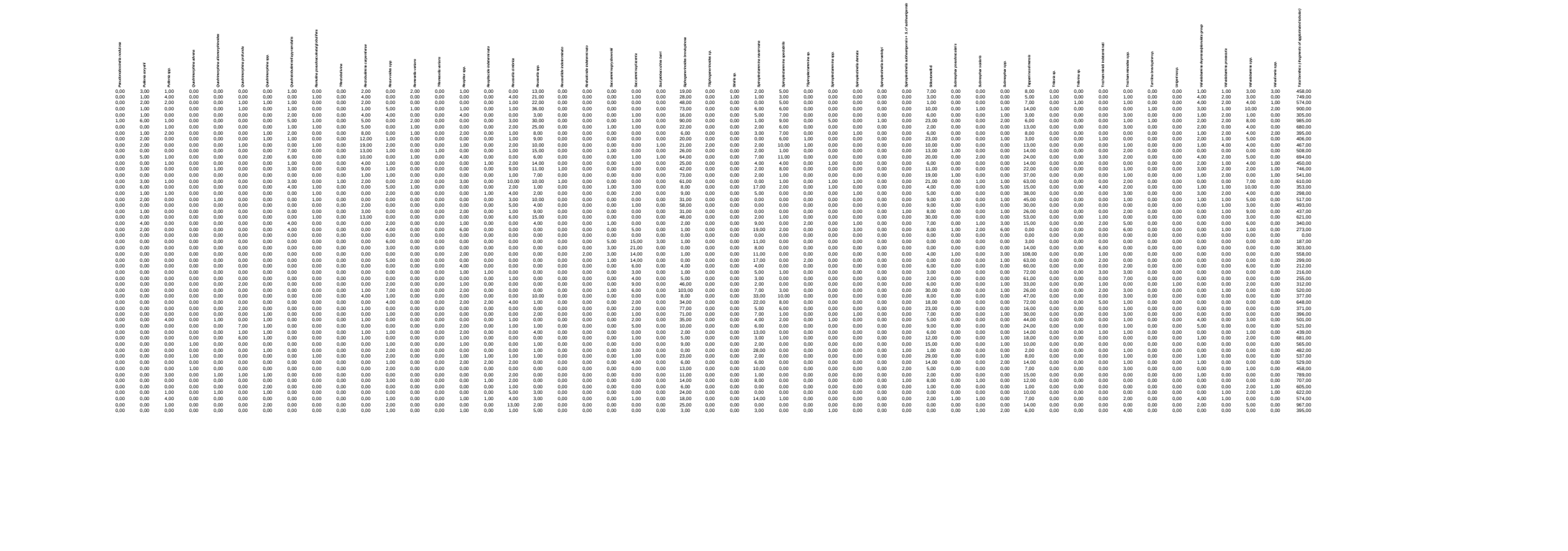

Table S2. Taxonomic list of benthic foraminiferal taxa recognized in the Paleocene-Eocene at Forada section*.

Agglutinant taxa

Ammobaculites agglutinans = Spirolina agglutinans d'Orbigny, 1846; **Plate II, fig. 1**
Ammobaculites spp.
Ammodiscus cretaceus = Operculina cretacea Reuss, 1845; **Plate IV, fig. 1**
Ammodiscus peruvianus Berry, 1928; **Plate IV, fig.2**
Ammodiscus tenuissimus Grzybowski, 1898
Ammodiscus spp.
Ammosphaeroidina pseudopauciloculata = Cystamminella pseudopauciloculata Mjatliuk, 1966
Arenobulimina spp.
Aschemocella grandis = Reophax grandis Grzybowski, 1896
Aschemocella cf. *moniliformis* Neagu, 1964
Aschemocella?
Caudammina ovuloides = Reophax ovuloides Grzybowski, 1901; **Plate IV, fig. 12**
Caudammina spp.
Cyclammina placenta = Nonionina placenta Reuss, 1851
Clavulinoides amorpha = Clavulina amorpha Cushman, 1926; **Plate I, fig. 21**
Clavulinoides globulifera = Pseudoclavulina globulifera ten Dam & Sigal, 1950; **Plate 1, fig. 19**
Clavulinoides trilatera Cushman, 1926; **Plate I, fig. 20**
Clavulinoides spp.
Dorothia beloides von Hillebrandt, 1962; **Plate I, fig. 23**
Dorothia pupa = Textularia pupa Reuss, 1860; **Plate I, fig. 24**
Dorothia retusa = Gaudryina retusa Cushman, 1926
Dorothia trochoides Marsson, 1878
Dorothia sp. (juvenile forms)
Dorothia spp.
Eobigenerina variabilis = Bigenerina variabilis Vašiček, 1947 in Cetean et al. (2011); **Plate II, fig. 2, 3**
Fragments of tubular agglutinants, belonging to:

- *Rhabdammina* spp.
- *Rhizammina* spp.
- *Bathysiphon* spp.

Gaudryina pyramidata Cushman, 1926; **Plate IV, fig. 13**
Gaudryina sp. with rectangular cross section; **Plate IV. fig. 10**
Gaudryina sp. with triangular cross section
Gaudryina sp.
Glomospira charoides = Trochammina squamata var. charoides Jones & Parker, 1860; **Plate II, fig. 13**
Glomospira diffundens Cushman & Renz, 1946
Glomospira gordialis = Trochammina squamata var. gordialis Jones & Parker, 1860; **Plate 4, fig. 9**
Glomospira irregularis = Ammodiscus irregularis Grzybowski, 1898; **Plate II, fig. 11**
Glomospira serpens = Ammodiscus serpens Grzybowski, 1898; **Plate IV, fig. 6**
Glomospira spp.
Haplophragmoides horridus = Haplophragmium horridum Grzybowski, 1901; **Plate IV, fig. 4**
Haplophragmoides stomatus /kirki/ porrectus group, includes:

- *Haplophragmoides stomatus* Grzybowski, 1898
- *Haplophragmoides kirki* Wickenden, 1932; **Plate II, fig. 9**
- *Haplophragmoides porrectus* Maslakova, 1955

Haplophragmoides walteri = Trochammina walteri Grzybowski, 1898; **Plate IV, fig. 3**
Haplophragmoides spp.
Hormosina velascoensis = Nodosinella velascoensis Cushman, 1926; **Plate IV, fig. 15**
Hormosina spp.
Hormosinid (indetermined)
Hyperammina spp.
Karrerulina coniformis = Gaudryina coniformis Grzybowski, 1898; **Plate IV, fig. 11**
Karrerulina conversa = Gaudryina conversa Grzybowski, 1901; **Plate II, Fig. 4**
Karrerulina horrida = Karreriella horrida Mjatlyuk, 1970; **Plate II, fig. 5**
Karrerulina spp.
Karrerotextularia sp.
Karrierella spp.
Lagenammina spp.
Lituotuba lituiformis = Trochammina lituiformis Brady, 1879
Lituolids; Big-size specimens (usually >500 μm) occurring exclusively in the Paleocene portion of the Forada section; **Plate IV, fig. 14, 20**
Marssonella indentata = Gaudryina indentata Cushman & Jarvis 1926; **Plate I, fig. 22**
Paratrochamminoides heteromorphus = Trochammina heteromorpha Grzybowski, 1898; **Plate IV, fig. 8**
Paratrochamminoides spp.
Psammosphaera spp.
"Pseudobolivinids" group, including:

- *Rashnovammina munda = Pseudobolivina munda* Krasheninnikov, 1973; **Plate II, fig. 8**
- *Bicazammina* spp.
- "*Pseudobolivina*" sp. 2 in Galeotti et al., 2004; **Plate IV, fig. 17**
- *Pseudobolivina* spp.

Pseudoclavulina trinitatensis Cushman & Renz 1948; **Plate IV, fig. 18**
Pseudoclavulina spp.
Pseudonodosaria spp.
Pseudonodosaria? sp.
Pseudonodosinella elongata = Reophax elongata Grzybowski, 1898
Pseudonodosinella nodulosa = Reophax nodulosa Brady, 1879 emend. Loeblich & Tappan, 1987
Pseudonodosinella troyeri = Reophax troyeri Tappan, 1960; **Plate IV, fig. 15**
Recurvoides cf. *walteri = Haplophragmium walteri* Grzybowski, 1898 emend. Mjatliuk, 1970
Recurvoides spp.
Remesella varians = Matanzia varians Glaessner, 1937; **Plate I, fig. 18**
Remesella? *varians*?
Reophax spp.
Reophacid indetermined
Rzehakinid indetermined
Saccammina grzybowski Schubert, 1902
Saccammina placenta = Reophax placenta Grzybowski,1898; **Plate II, Fig. 10**
Sculptobacculites barri Beckmann, 1991
Spiroplectammina navarroana Cushman, 1932; **Plate 2, Fig. 6**
Spiroplectammina spectabilis = Spiroplecta spectabilis Grzybowski, 1898 emend. Kaminski, 1984; **Plate II, fig. 7 and Plate IV, fig. 19**
Spiroplectinella israelskyi Von Hillebrandt, 1962
Spiroplectinella subhaeringensis = Textularia subhaeringensis Grzybowski,1896
Spiroplectammina spp.
Spiroplectammina? sp.
Subreophax pseudoscalaris = Reophax pseudoscalaria Samuel, 1977

Subreophax scalaris = Reophax guttifera Grzybowski, 1896
Subreophax spp.
Trochamminids. Intermediate forms between *Trochamminoides* e *Paratrochamminoides.*
Trochamminoides proteus = Trochammina proteus Karrer, 1866 *sensu* Rögl, 1955; **Plate IV, fig. 7**
Trochamminoides spp.

Porcellaneous taxa
Miliolids

Calcareous-hyaline taxa
Abyssammina incisa Schnitker & Tjalsma, 1980
Abyssammina cf. *incisa* Schnitker & Tjalsma, 1980
Abyssammina poagi Schnitker & Tjalsma, 1980; **Plate II fig. 26**
Abyssammina quadrata Schnitker & Tjalsma, 1980
Abyssammina spp.
Alabamina midwayensis Brotzen, 1948
Alabamina spp.
Allomorphina trochoides = Globigerina trochoides Reuss, 1845; **Plate III, fig. 18**
Allomorphina sp.
Angulogavelinella avnimelechi = Pseudovalvulineria avnimelechi Reiss, 1952; **Plate I, fig. 1, 2**
Angulogerina muralis = Uvigerina muralis Terquem, 1882; **Plate III, fig. 13, 14**
Angulogerina? sp.; **Plate III, fig. 15, 16.**
Angulogerina spp.
Angulogerinid indetermined
Anomalinoides rubiginosus = Anomalina rubiginosa Cushman, 1926; **Plate I, fig. 5**
Anomalinoides sp. 1; Small-size anomalinid with low trochospiral coiling, strongly compressed, not biumbilicate, fourteen chambers in the last whorl, smooth. It occurs exclusively within the CMU interval at Forada.
Anomalinoides sp. 2; Small-size anomalinid with low trochospiral coiling, with a spiral side showing an elevated spiral suture and small costae along the suture lines. It occurs exclusively in the Paleocene portion of the Forada section; **Plate III, fig. 21**
Anomalinoides spp.
Aragonia aragonensis = Textularia aragonensis Nuttall, 1930; **Plate II, fig. 25**
Aragonia velascoensis = Textularia velascoensis Cushman, 1925; **Plate I, fig. 14**
Astacolus spp. group, includes:

- *Saracenaria* spp.
- *Astacolus* spp.
- *Planularia* spp.

Bolivina spp. smooth; **Plate III, fig. 10, 11**
Bolivina spp. with costae; **Plate II, fig. 22**
"Bolivina" sp. A; bolivinid with an initial biserial coiling followed by triserial coiling
Bolivina? sp.
Bolivinoides crenulata group, includes:

- *Bolivinoides crenulata= Bolivina crenulata* Cushman, 1936; **Plate III, fig. 7,8**
- *Bolivina floridana* Cushman, 1918; **Plate III, fig. 9**

Bolivinoides delicatulus Cushman, 1927; **Plate I, fig. 15**
Bolivinoides cf. *delicatulus* Cushman, 1927
Bulimina alazanensis Cushman, 1927; **Plate III, fig. 4**
Bulimina callahani Galloway & Morrey, 1931
Bulimina kugleri Cushman & Renz, 1942
Bulimina cf. *kugleri* Cushman & Renz, 1942

Bulimina midwayensis group, includes:

- *Bulimina midwayensis* Cushman & Parker, 1936; **Plate III, fig. 3**
- *Bulimina macilenta* Cushman & Parker, 1939
- *Bulimina* cf. *macilenta* Cushman & Parker, 1939

Bulimina semicostata Nuttall, 1930
Bulimina trihedra Cushman, 1926
Bulimina cf. *trihedra* Cushman, 1926
Bulimina trinitatensis Cushman & Jarvis, 1928; **Plate III, fig. 5, 6**
Bulimina tuxpamensis Cole, 1928; **Plate II, fig. 19, 20**
Bulimina sp. 1; small-size buliminid comparable to the genera *Buliminella*, *Sitella* and *Praebulimina*
Bulimina sp. 2
Bulimina spp.
Buliminella grata Parker & Bermudez, 1937
Buliminella spp.; **Tavola 2, Fig. 2**
Cibicids; **Plate III, fig. 22**
Cibicidoides dayi = Planulina dayi White, 1928; **Plate I, fig. 6**
Cibicidoides eocaenus = Rotalia eocaena Gümbel, 1868 *sensu* van Morkhoven et al., 1986; **Plate III, fig. 20**
Cibicidoides hyphalus = Anomalinoides hypalus Fisher, 1969; **Plate I, fig. 9**
Cibicidoides praemundulus Berggren & Miller, 1986; **Plate III, fig. 23**
Cibicidoides cf. *pseudoperlucidus = Cibicides (Gemellides) pseudoperlucidus* Bykova, 1954 in Tjalsma and Lohmann, 1983
Cibicidoides velascoensis = Anomalina velascoensis Cushman, 1925; **Plate I, fig. 7, 8**
Cibicidoides spp.
Coryphostoma midwayensis = Bolivina midwayensis Cushman, 1936; **Plate I, fig. 13**
Coryphostoma? sp.; small-size biserial forms with several chambers comparable to *Coryphostoma* and occurring exclusively in the lower Eocene portion of the study section
Dentalina spp.; we include both smooth and costate forms (*Laevidentalina* and *Dentalina sensu* Loeblich & Tappan, 1987)
Ellipsoglandulina spp.
Ellipsoidina
Ellipsopolymorphina
Ellipsopolymorphina?
Eouvigerina sp.
Eponides sp.
Eponides? sp
Fursenkoina sp.
Gavelinella beccariiformis = Rotalia beccariiformis White, 1928; **Plate I, fig. 3**
Globocassidulina subglobosa = Cassidulina subglobosa Brady, 1881; **Plate II, fig. 14** (dwarfed specimen)
Globorotalites spp.
Gyroidinoides globosus = Nonionina globosa Hagenow, 1842 emend. Alegret & Thomas (2001); **Plate I, fig. 11**
Gyroidinoides quadratus = Gyroidina quadrata Cushman &Church, 1929; **Plate I, fig. 12**
Gyroidinoides subangulatus = Rotalia soldanii Plummer, 1926
Gyroidinoides spp.
Hanzawaia ammophila = Rotalia ammophila Gümbel, 1868
Hanzawaia spp.
Indetermined trochospiral hyalineous. Group including small size, badly preserved and indeterminable low trochospiral forms.
Lagenid indeterminate

Lenticulina spp. (smooth-walled)
Loxostomid indeterminate
Neoflabellina jarvisi = Flabellina jarvisi Cushman, 1935
Neoflabellina semireticulata = Flabellina semireticulata Cushman & Jarvis, 1928; **Plate I, fig. 16**
Neoflabellina sp.
"Neoeponides" megastoma = Pulvinulina megastoma Grzybowski, 1896; **Plate 1, fig. 10**
Nodosarella spp.
Nodosaria/Chrysalogonium group, includes the genera:

- *Nodosaria* spp.
- *Pyramidulina* spp.
- *Chrysalogonium* spp.

Nodosariid (indeterminate)
Nonion havanense Cushman & Bermudez, 1937; **Plate III, fig. 24**
Nonion spp.
Nonionella spp.
Nonionids (indeterminate)
Nuttallides truempyi = Eponides truempyi Nuttall, 1930; **Plate II, fig. 23**
Nuttallinella florealis = Gyroidina florealis White, 1928
Oridorsalis cf. *plummerae = cf. Eponides plummerae* Cushman, 1948
Oridorsalis umbonatus = Rotalina umbonata Reuss, 1851; **Plate II, fig. 24**
Oridorsalis cf. *umbonatus* (Reuss, 1851)
Oridorsalis sp.
Oridorsalis? sp.
Orthomorphina spp.
Osangularia velascoensis = Truncatulina velascoensis Cushman, 1926; **Plate I, fig. 4**
Osangularia spp. small-size; **Plate 2, fig. 13**
Paleopolymorphina spp.
Paralabamina hillebrandti = Neoeponides hillebrandti Fisher, 1969
Pyramidina europaea = Angulogerina europaea Cushman & Edwards, 1937
Pleurostomella spp.; **Plate 2, fig. 22**
Pleurostomellids
Polymorphinids
Praebulimina spp.
Protoelphidium? sp.
Pullenia coryelli White, 1929; **Plate I, fig. 17.**
Pullenia cretacea Cushman, 1936
Pullenia jarvisi Cushman, 1936
Pullenia paleocenica Brotzen, 1948 emend. Pozaryska, 1965
Pullenia quinqueloba Reuss, 1951
Pullenia spp.
Quadratobuliminella pyramidalis de Klasz, 1953; **Plate III, fig. 1**
Quadrimorphina advena = Valvulineria advena Cushman & Siegfus, 1939
Quadrimorphina allomorphinoides = Valvulina allomorphinoides Reuss, 1860; **Plate III, fig. 19**
Quadrimorphina profunda Schnitker & Tjalsma, 1980
Quadrimorphina spp.
Ramulina pseudoaculeata Olsson, 1960
Rectobulimina carpentierae Marie, 1956; **Plate II, fig. 17**
Recurvoides anormis Mjatliuk, 1970
Reussella cimbrica = Pseudouvigerina cimbrica Troelsen, 1945
Reussella spp.
Reussellid indeterminate

Siphogenerinoides brevispinosa Cushman, 1939; **Plate II, fig. 17, 18**
Siphogenerinoides? sp.
Sitella? sp.
Stilostomellids (include genera *Siphonodosaria* and *Stilostomella*)
Tappanina selmensis = Bolivinita selmensis Cushman, 1933 emend. Brotzen, 1948; **Plate II, fig. 15, 16**
Trifarina sp.
Turrilina brevispira Ten Dam, 1944
Turrillina sp.
Unilocular forms
Biserials indeterminate
Uvigerina sp.
Uvigerina?
Valvalabamina depressa/planulata group, includes:

- *Valvalabamina depressa = Rotalina depressa* Alth, 1850
- *Valvalabamina planulata = Gyroidina planulata* Cushman & Renz, 1941

Valvalabamina praeacuta = Anomalina preacuta Vasilenko, 1950
Valavalabamina spp.
Valvulineria spp.

*Note: benthic foraminiferal taxa were identified mainly following the taxonomy outlined in the papers cited in the reference list below.

References

Alegret, L. and Thomas, E., 2001. Upper Cretaceous and lower Paleogene benthic foraminifera from northeastern Mexico. Micropaleontology, 47, 269-316.

Berggren, W.A. and Aubert, J., 1975. Paleocene benthonic foraminiferal biostratigraphy, paleobiogeography and paleoecology of Atlantic-Tethyan regions: Midway-type fauna. Palaeogeography, Palaeoclimatology, Palaeoecology, 18, 73-192.

Bolli, H.M., Beckman, J.P., and Saunders, J.B., 1994. Benthic foraminifera biostratigraphy of the south Caribbean region. Cambridge University Press, 408 pp.

Braga, G., De Biase, R., Gruning, A., and Proto Decima, F., 1975. Foraminiferi bentonici del Paleocene e dell'Eocene della sezione di Possagno. In Bolli H.M. (ed.), Monografia micropaleontogica sul Paleocene e l'Eocene di Possagno, Provincia di Treviso, Italia. Schweizerische Paläontologische Abhandlungen, 97, 85-111.

Cetean, C.G., Setoyama, E., Kaminski, M., Neagu, T., Bubík, M., Filipescu, S., and Tyszka, J., 2011. *Eobigenerina* a cosmopolitan deep-water agglutinated foraminifer, and remarks on late Paleozoic to Mesozoic species formerly assigned to *Pseudobolivina* and *Bigenerina*. In Kaminski M.A. & Filipescu S. (eds.), Proceedings of the Eighth International Workshop on Agglutinated Foraminifera. Gryzbowski Foundation Special Publication, 16, 19-27.

Galeotti, S., Kaminski, M.A., Coccioni, R., and Speijer, R., 2004. High-resolution deep water agglutinated foraminiferal record across the Paleocene/Eocene transition in the Contessa Road Section (central Italy). In Bubik M., Kaminski, M.A. (Eds.), Proceedings of the Sixth International Workshop on Agglutinated Foraminifera. Grzybowski Foundation Special Publication, 8, 83–103.

Kaminski, M.A. and Geroch, S., 1993. A revision of foraminiferal species in the Grzybowski collection. In Kaminski M.A., Geroch S., Kaminski D.G. (eds.), The origin of applied micropaleontology: the school of Jòzef Grzybowski. Grzybowski Foundation Special Publication, 1, 239-323, Alden Press.

Kaminski, M.A. and Gradstein, F.M., 2005. Atlas of Paleogene Cosmopolitan Deep-water Agglutinated Foraminifera. Gryzbowski Foundation Special Publication, 10, 547 pp. + vii pp.

Kaminski, M.A., Kuhnt, W.A., and Radley, J.D., 1996. Paleocene-Eocene deep-water agglutinated foraminifera from the Namibian Flysch (Rif., Northern Morocco): Their significance for the palaeoceanography of the Gibraltar Gateway. Journal of Micropalaeontology, 15, 1-19.

Kuhnt, W., 1990. Agglutinated foraminifera of western Mediterranean Upper Cretaceous pelagic limestones (Umbria Appennines, Italy and Betic Cordillera, Southern Spain). Micropaleontology, 36, 297-330.

Loeblich, A.R. and Tappan, J.H., 1987. Foraminiferal genera and their classification. 970 pp. (2 vol.), Van Nostrand Reinhold.

Loeblich A.R. and Tappan H., 1992. Present status of foraminiferal classification. In Takayanagi Y. & Saito T. (eds.), Proceedings of the Fourth International Symposium on benthic Foraminifera, Sendai, 1990 (Benthos '90). Tokyo University Press, Tokyo, 93-102.

Ortiz, S. and Thomas, E., 2006. Lower-middle Eocene benthic foraminifera from the Fortuna Section (Betic Cordillera, southeastern Spain). Micropaleontology, 52, 97-150.

Speijer, R.P. and Van Der Zwaan, G.J., 1994. Extinction e survivorship patterns in southern Tethyan bentic foraminiferal assemblages across the Cretaceous/Paleogene and Paleocene/Eocene boundaries. Geologica Ultraiectina, 124, 16-64.

Speijer, R.P. and Van Der Zwaan, G.J., 1994b. The impact of Paleocene/Eocene boundary events on middle neritic benthic foraminiferal assemblages from Egypt. In Speijer R.P., Extinction and recovery patterns in benthic foraminiferal paleocommunities across the Cretaceous/Paleogene and Paleocene/Eocene boundaries. Geologica Ultraiectina, 124, 91-120.

Sztràkos, K., 2005. Paleocene and lowest Eocene foraminifera from the North Pyrenean trough (Aquitane, France). Revue de Micropaleontologie, 48, 175-236.

Tjalsma, R.C. and Lohmann, G.P., 1983. Paleocene-Eocene bathyal and abyssal benthic foraminifera from the Atlantic Ocean. Micropaleontology Special Publication, 4, 90 pp.

Van Morkhoven, F.P.C.M., Berggren, W.A., and Edwards, A.S., 1986. Cenozoic cosmopolitan deep-water benthic foraminifera. Bullettin des Centres de Recherches Exploration-Production Elf-Aquitane, Mèmoire, 11, 11-421.

Von Hillebrandt, A., 1962. Das Paläozän und seine Foraminiferenfauna im Becken von Reichenhall und Salzburg. Bayerische Akademie der Wissenschaften, Mathematisch-Naturwissenschaftliche Klasse, Abhandlungen, Heft 108, 9-180.

Widmark, J.G.V. and Speijer, R.P., 1997. Benthic foraminiferal ecomarker species of the terminal Cretaceous (late Maastrichtian) deep-sea Tethys. Marine Micropaleontology, 31, 135-155.

Table S3. Summary of the localities where paleohydrological reconstructions for the PETM are available and of the proxies used to infer hydrological changes. Numbers follow the same north to south paleolatitudinal order as in text Figure 10.

Location	Paleolatitude	δD	Clay minerals	Paleobotany	Marine microfossils	Lithological anomalies and/or sedimentological changes	Inferred paleohydrology at the PETM	References
(1) Central Arctic Ocean	~90°N	Positive excursion at the onset of the PETM (-220 to -160‰);	NA	Rise in angiosperm pollen, decline in gymnosperms and fern palynomorphs.	*Apectodinium* acme; low-salinity, eutrophy tolerant dinocysts; benthic foraminifera barren.	Sediment lamination, peak in isorenieratene.	Enhanced precipitations in the Arctic region, leading to increased runoff and water column stratification.	Pagani et al., (2006). Sluijs et al., (2006).
(2) Spitsbergen Central Basin (marine)	75°N	NA	Kaolinite decrease.	No vegetation changes, but increased fern spores.	*Apectodinium* acme; Low-salinity dinocysts (*Senegalinium*); benthic foraminifera linings.	Sediment lamination, increase in pyrite and in amorphous organic matter.	Increased stratification due to increased regional precipitations and runoff; eustatic sea-level rise.	Harding et al., (2011).
(3) Svalbard archipelago	75°N	NA	Kaolinite increase.	NA	*Apectodinium* acme.	Laminated pyrite-rich beds, with low Th/U values.	Increased in chemical weathering due to enhanced precipitations.	Sluijs et al. (2006); Dypvik et al. (2011).
(4) Central North Sea Basin (marine)	55°N	NA	Kaolinite increase.	Palynomorphs indicate coastal swamp conifers replaced by generalists as alders, ferns, and fungi; early CIE diverse angiosperm and pteridophyte vegetation.	*Apectodinium* acme. Increase in low-salinity and eutrophy tolerant dinocysts. benthic foram barren.	increased organic matter C/N ratio.	Increased regional precipitations and runoff; Warm and wetter summers just prior and during the PETM.	Bujak and Brinkhuis, (1998); Knox, (1998); Kender et al., (2012); Elderett et al. (2014).
(5) Eastern North Sea Basin (marine)	~50°N	NA	NA	Increased pollens from a freshwater or lowland environment; appearance of paratropical elements, and increase in herb pollens.	*Apectodinium* acme.	Increase in organic matter (OM) and pyrite.	Increased precipitations and runoff; increased seasonality.	Nielsen et al. (1985); Heimann-Clausen, (1994); Beerling and Jolley, (1998); Heimann-Clausen and Schmitz, (2000); Willimusen et al. (2014); Schoon et al. (2015).
(6) Williston Basin, Western North Dakota (USA) (continental)	47°N	NA	Kaolinite increase.	Little floral changes.	NA	Shift from mudstones to the kaolinite rich Bear Den Member of the Golden Valley Formation.	Intese chemical weathering, variable hydrological conditions with cycles of wetting and drying.	Harrington et al., (2005); Clechenko et al., (2007).
(7) Bighorn Basin, Wyoming (USA) (continental)	45°N	Positive shift at the onset of the PETM (13‰), subsequent negative shift at the main CIE (-17‰); PETM average -190‰.	NA	Fossil plants, palynomorphs, along with n-alkane δ13C, indicate a floral change toward an angiosperm dominated plant community.	NA	Tight alternation of different kind of paleosols and avulsion deposits.	Variable hydrological conditions during the PETM, cycles of wetting and drying possibly precessionally paced.	Wing et al. (2005); Smith et al. (2007); Krauss and Riggins (2007); Aziz et al. (2008); Kraus et al. (2013); Woody et al. (2014).
(8) Rhenodanubian Basin (Anthering and Untersberg sections, Austria) (marine)	45°N	NA	No changes in clay mineral assemblage.	NA	NA	Shift from marlstones to a 5 m red claystone interval; doubling of quarz and feldspare at the onset of the CIE.	Increased mechanical erosion on the continent due to alternate, pronounced dry and wet seasons.	Egger et al. (2003; 2005; 2009).
(9) Belluno Basin (Forada and Cicogna sections, Italy) (marine)	45°N	Pre-CIE positive shift at Forada (+20‰), subesequent negative shift at the PETM (-20‰; average within the CIE -145‰); Negative shift at the PETM at Cicogna (-10‰).	No changes in clay assemblage.	Decreased n-alkane average chain lenght within the CIE might indicate plant community changes.	Benthic foraminifera (Forada) indicate a fluctuating high primary productivity during the PETM.	Shift from marlstones to a >3.5 m thick clay rich interval; Increase in quartz%; peaks of hematite.	Intense erosion on land, variable hydrological conditions with cycles of wetting and drying.	Giusberti et al. (2007); Tipple et al. (2011), Krishna et al. (2015); present paper.
(10) Aktumsuk (Uzbekistan, continental) and Kaurtakapy (Kazakhstan, marine)	45°N	NA	No changes in clay assemblage.	NA	NA	Throughout the lowermost Eocene decrease in CaCO3%, increase in clay content, quarz, feldspare, plagioclase.	Onset of a phase of more humid sesonal climate.	Bolle et al. (2000b).
(11) Dieppe-Hampshire Basin, North Normandie (France) (terrestrial to marine)	~40°N	Negative excursion of about 60‰ at the PETM (-110/-112 to -174/185‰).	NA	NA	*Apectodinium* acme.	Increase in organic matter (OM); change in OM type.	Moister conditions along with a stronger seasonality during the lowermost PETM.	Storme et al. (2012); Garel et al. (2013).
(12) London Basin, South-easter England (continental)	~40°N	NA	NA	NA	NA	Inertinite-rich–inertinite-poor layering.	Persistent fire regime with regular dryer intervals followed by rainfall and runoff events.	Collison et al. (2007; 2009).
(13) DSDP Site 401	~40°N	NA	Kaolinite increase.	NA	NA	Shift from calcareous nannofossil chalks to a clay rich unit.	Increased physical weathering on land due increased precipitations, with pronounced dry and wet periods.	Bornemann et al. (2014).
(14) Western Colorado	~40°N	NA	NA	NA	NA	Larger fluvial channels and preservation of upper-flow-regime structures.	Increased discharge due to greater rainfalls, possibly seasonal or monsoonal.	Foreman et al., (2012).
(15) New Jersey coastal plain (USA) (shallow marine)	~40°N	NA	Kaolinite increase.	NA	*Apectodinium* acme; *Apectodinium* anticovariant with low-salinity, eutrophy tolerant dynocists (*Senegalinium*); benthic foraminifera point to dysoxic sea-floor at the PETM onset, later to seasonal stratification.	Shift from glauconitic-sandy strata to the kaolinite-rich Marlboro formation; increase in magnetofossils.	Dynamic climate state, more extreme water cycle, with long dry seasons, enhanced erosion and sediment transport; eustatic sea-level rise.	Gibson et al., (2000); Zachos et al., (2006); Sluijs et al., (2007); Kopp et al., (2009); Sluijs and Brinkhuis, (2009); John et al., (2008; 2012); Stassen et al., (2012a,b; 2015).

Location	Paleolatitude	δD	Clay minerals	Paleobotany	Marine microfossils	Lithological anomalies and/or sedimentological changes	Inferred paleohydrology at the PETM	References
(16) Central Valley of California (USA) (shallow marine)	35°N	NA	NA	NA	NA	Inrease in CaCO3% at the PETM, increased sediment accumulation rates.	Increase in physical weathering due to changes in the hydrological cycle.	John et al., (2008).
(17) Basque Basin (Zumaia, Trabakua pass, Ermua sections), Northern Spain (marine);	~35°N	NA	Kaolinite increase.	Pollens suggest a shift from permanent conifer forests to a periodic vegetation with mostly angiosperms and ferns.	NA	Shift from hemipelagic marls and limestones to carbonate-free, clay rich units.	Increased mechanical erosion on the continent due to increasing seasonal aridity alternate with rainy periods.	Bolle et al. (1998); Schmitz et al. (2001).
(18) Tremp Basin, Northern Spain (continental);	~35°N	NA	Smectite increase.	NA	NA	Increase in clay content; Claret Conglomerate at the base of the CIE.	Shift from arid to seasonally wetter but still generally dry conditions; episodic flash floods at the onset of the PETM.	Schmitz and Pujalte (2003; 2007).
(19) Alamedilla section, Southern Spain (marine)	30°N	NA	Palygorskite increase.	NA	NA	Gradual shift from grey marls to a red clay interval; Increased terrestrial sediment deposition.	Increased aridity on continent, increased continental erosion.	Lu et al. (1998); Arreguín-Rodríguez et al. (2014).
(20) Tornillo Basin, Texas (USA) (continental)	30°N	NA	Kaolinite increase.	NA	NA	Shift from red to black paleosols with no carbonates.	Increased humidity and rainfalls.	White et al. (2008).
(21) Salisbury Embayment, (USA) (shallow marine)	~30°N	NA	Kaolinite increase.	NA	NA	Shift from sandy-silty lithologies to the kaolinite-rich Marlboro formation; increase in magnetofossils.	Increase in weathering due to changes in the hydrological cycle.	Gibson et al., (2000); Kopp et al., (2009).
(22) Gafsa Basin (Tunisia) (shallow marine)	~20°N	NA	Palygorskite and sepiolite increase.	NA	NA	No lithological changes.	Major seasonal aridity with enhanced evaporation in continental areas.	Bolle et al. (1999).
(23) Zin Valley of Negev (Ben Gurion I, II and Zomet Telalim sections, Israel) (marine)	~20°N	NA	Palygorskite and sepiolite increase.	NA	NA	No lithological changes.	Major seasonal aridity with enhanced evaporation in continental areas.	Bolle et al. (2000a).
(24) Dababiya section, Egypt (shallow marine)	~15°N	NA	Increase in chlorite.	NA	NA	Shift from marls to non-calcareous laminated clays.	Perennial humid continental conditions at the onset of the CIE; More seasonal fluctuating (arid) climate coinciding with the middle to uppermost CIE.	Ernst et al. (2006); Schulte et al. (2011).
(25) Northern Neotropics (Colombia and Venezuela) (continental)	~10°N	Negative shift (35‰) at the onset of the PETM	NA	Pollens indicate increased plant diversity and abundance of angiosperms.	NA	No lithological changes.	High rate of precipitations.	Jaramillo et al. (2010).
(26) TDP Site 14, Tanzania (shallow marine)	~20°S	Positive shift at the onset of the PETM (+15-40‰)	Increase in kaolinite.	No floral changes.	NA	No lithological changes.	Increased aridity with intense periodical precipitations.	Handley et al. (2008; 2012).
(27) Tawanui section, North Island (New Zealand) (marine)	~45°S	NA	Increases in kaolinite/illite and kaolinite/smectite ratios.	Pollens indicative of conifer-dominated rainforests; no major changes at the PETM; increase in terrestrial palynomorphs.	*Apectodinium* acme.	Increase in TOC%, C/N, SiO2, Al2O3.	Increase in terrestrial weathering and runoff.	Kaiho et al., (1996); Crouch and Visscher, (2003); Crouch et al., (2003).
(28) Clarence River valley, South Island (New Zealand) (marine)	~55°S	NA	NA	NA	NA	Shift from limestone to clay rich marls (recessive unit).	Increase in terrestrial weathering and runoff.	Hancock et al. (2003); Hollis et al. (2005); Nicolo et al. (2007; 2010); Slotnick et al. (2012).
(29) Central Westland, South Island (New Zealand) (terrestrial to shallow marine)	~55°S	Negative and positive fluctuations of about ±20‰ across the PETM (-140 - 160‰)	NA	Pollens and oleanane suggest the transitional development of mangrove swamps.	*Apectodinium* acme.	Shift from shales to dark mudstones with pyrite; increased terrigenous biomarkers.	Eustatic sea level rise, possibly increased sesonality in precipitations.	Sluijs et al. (2008); Handley et al. (2011).
(30) ODP Site 1172, East Tasman Palteau (shallow marine)	65°S	NA	NA	Increase in terrestrial palynomorphs.	*Apectodinium* acme; increasing abundances of normal marine taxa among dynocists, with a peak in the euryhaline taxon *Eocladopyxis*.	No lithological changes.	Eustatic sea level rise, possibly increased sesonality in precipitations.	Sluijs et al. (2011).
(31) ODP Site 690, Weddell Sea	65°S	NA	Increase in kaolinite.	NA	NA	No lithological changes.	Increased precipitations.	Robert and Kennett (1994).

References

Abdul Aziz, H., Hilgen, F.J., van Luijk, G.M., Sluijs, A., Kraus, M.J., Pares, J.M., and Gingerich, P.D., 2008. Astronomical climate control on paleosol stacking patterns in the upper Paleocene-lower Eocene Willwood Formation, Bighorn Basin, Wyoming. Geology, 36, 531–534.

Arreguín-Rodríguez, G.J., Alegret, L., Sepúlveda, J., Newman, S., and Summons, R.E., 2014. Enhanced terrestrial input supporting the *Glomospira* acme across the Paleocene-Eocene boundary in Southern Spain. Micropaleontology, 60, 43-51.

Beerling, D.J. and Jolley, D.W., 1998. Fossil plants record an atmospheric $^{12}CO_2$ and temperature spike across the Paleocene-Eocene transition in NW Europe. Journal of the Geological Society, London, 155, 591–594.

Bolle, M.P., Adatte, T., Keller, G., von Salis, K., and Hunziker, J., 1998. Biostratigraphy, mineralogy and geochemistry of the Trabakua Pass and Ermua sections in Spain. Eclogae Geologicae Helvetiae, 91, 1–25.

Bolle, M.P., Adatte, T., Keller, G., von Salis, K., and Hunziker, J., 1999. The Paleocene-Eocene transition in the southern Tethys (Tunisia): climatic and environmental fluctuations. Bulletin de la Société géologique de France, 170, 661-680.

Bolle, M.-P., A. Pardo, T. Adatte, K. Von Salis, and S. Burns 2000a. Climatic evolution on the southeastern margin of the Tethys (Negev, Israel) from the Palaeocene to the early Eocene: Focus on the late Paleocene thermal maximum. Journal of the Geological Society of London, 157, 929–941.

Bolle, M.P., Pardo, A., Hinrichs K.U., Adatte, T., Von Salis, K., Burns, S., Keller G., and Muzylev N., 2000b. The Paleocene-Eocene transition in the marginal northeastern Tethys. International Journal of Earth Sciences, 89, 390-414.

Bornemann, A., Norris, R.D., Lyman, J.A., D'haenens, S., Groeneveld, J., Röhl, U., Farley, K.A., and Speijer, R.P., 2014. Persistent environmental change after the Paleocene–Eocene Thermal Maximum in the eastern North Atlantic. Earth and Planetary Science Letters, 394, 70–81.

Bujak, J. and Brinkhuis, H., 1998. Global warming and dinocyst changes across the Palaeocene/Eocene epoch boundary. In: Aubry, M.-P., Lucas, S.G., Berggren, W.A. (Eds.). Late Palaeocene–Early Eocene Biotic and Climatic Events in Marine and Terrestrial Records. Columbia Univ. Press, New York, 277–295.

Clechenko, E.R., Kelly, D.C., Harrington, G.J., and Stiles, C.A., 2007. Terrestrial records of a regional weathering profile at the Paleocene-Eocene boundary in the Williston Basin of North Dakota. Geological Society of America Bulletin, 119, 428-442.

Collinson, M.E., Steart, D.C., Scott, A.C., Glasspool, I.J., and Hooker, J.J., 2007. Episodic fire, runoff and deposition at the Palaeocene–Eocene boundary. Journal of the Geological Society 164, 87–97.

Collinson, M.E., Steart, D.C., Harrington, G.J., Hooker, J.J., Scott, A.C., Allen, L.O., Glasspool, I.J., and Gibbons, S.J., 2009. Palynological evidence of vegetation dynamics in response to palaeoenvironmental change across the onset of the Paleocene-Eocene Thermal Maximum at Cobham, Southern England. Grana, 48 (1), 38-66.

Crouch, E.M. and Visscher, H., 2003. Terrestrial vegetation record across the initial Eocene thermal maximum at the Tawanui marine section, New Zealand. Geological Society of America Special papers, 369, 351-363.

Crouch, E.M., Dickens, G.R., Brinkhuis, H., Aubry, M.P., Hollis, C.J., Rogers, K.M., and Visscher, H., 2003. The Apectodinium acme and terrestrial discharge during the Paleocene-Eocene thermal maximum: New palynological, geochemical and calcareous nannoplankton observations at Tawanui, New Zealand. Palaeogeography Palaeoclimatology, Palaeoecology, 194, 387–403.

Egger, H., Heilmann-Clausen, C., and Schmitz, B., 2009. From shelf to abyss: Record of the Paleocene/Eocene-boundary in the Eastern Alps (Austria). Geologica Acta, 7 (1-2), 215-227.

Egger, H., Homayoun, M., Huber, H., Roegl, F., and Schmitz, B., 2005. Early Eocene climatic, volcanic, and biotic events in the northwestern Tethyan Untersberg section, Austria. Palaeogeography, Palaeoclimatology, Palaeoecology, 217, 243– 264.

Egger, H., Fenner, J., Heilmann-Clausen, C., Roegl, F., Sachsenhofer, R.F., and Schmitz, B., 2003. Paleoproductivity of the northwestern Tethyan margin (Anthering section, Austria) across the Paleocene–Eocene transition. Special Paper-Geological Society of America, 369, 133–146.

Eldrett J.S., Greenwood D.R., Polling M., Brinkhuis H., Sluijs A., 2014. A seasonality trigger for carbon injection at the Paleocene–Eocene Thermal Maximum. Climate of the Past, 10, 759–769.

Ernst, S.R., Guasti, E., Dupuis, C., and Speijer, R.P., 2006. Environmental perturbation in the southern Tethys across the Paleocene/Eocene boundary (Dababyia, Egypt): Foraminiferal and clay minerals record. Marine Micropaleontology, 60, 89-111.

Garel, S., Schnyder, J., Jacob, J., Dupuis, C., Boussafir, M., Le Milbeau, C., Storme, J.-Y., Iakovleva, A.I., Yans J., Baudin, F., Fléhoc, C., and Quesnel, F., 2013. Paleohydrological and paleoenvironmental changes recorded in terrestrial sediments of the Paleocene–Eocene boundary (Normandy, France). Palaeogeography, Palaeoclimatology, Palaeoecology, 376, 184–199.

Giusberti, L., Rio, D., Agnini, C., Backman, J., Fornaciari, E., Tateo, F., and Oddone, M., 2007. Mode and tempo of the Paleocene-Eocene Thermal Maximum in an expanded section from the Venetian pre-Alps. Geological Society of America Bulletin, 119, 391-412.

Hancock, H.J.L., Dickens, G.R., Strong, C.P., Hollis, C.J., and Field, B.D., 2003. Foraminiferal and carbon isotope stratigraphy through the Paleocene–Eocene transition at Dee Stream, Marlborough, New Zealand. New Zealand Journal of Geology and Geophysics, 46, 1–19.

Handley, L., Crouch, E.M., and Pancost, R.D., 2011. A New Zealand record of sea level rise and environmental change during the Paleocene–Eocene Thermal Maximum. Palaeogeography, Palaeoclimatology, Palaeoecology, 305, 185-200.

Handley, L., Pearson, P.N., McMillan, I.K., and Pancost, R.D., 2008. Large terrestrial and marine carbon and hydrogen isotope excursions in a new Paleocene/Eocene boundary section from Tanzania. Earth and Planetary Science Letters, 275, 17–25.

Handley, L., O'Halloran, A., Pearson,P.N., Hawkins, E., Nicholas, C.J., Schouten, S., McMillan, I.K., and Pancost, R.D., 2012. Changes in the hydrological cycle in tropical East Africa during the Paleocene–Eocene Thermal Maximum. Palaeogeography, Palaeoclimatology, Palaeoecology, 329–330, 10–21.

Harding, I.C., Charles, A.J., Marshall, J.E.A., Pälike, H., Roberts, A.P., Wilson, P.A., Jarvis, E., Thorne, R., Morris, E., Moremon, R., Pearce, R.B., and Akbari, S., 2011. Sea-level and salinity fluctuations during the Paleocene–Eocene thermal maximum in Arctic Spitsbergen. Earth and Planetary Science Letters, 303, 97–107.

Harrington, G.J., Clechenko, E.R., and Kelly, D.C., 2005, Palynological and geochemical records of change across a terrestrial Palaeocene/Eocene boundary section in the Williston Basin, North Dakota, USA. Palaeogeography, Palaeoclimatology, Palaeoecology, 226, 214–232, doi: 10.1016/j.palaeo.2005.05.013.

Heilmann-Clausen, C., 1995. Palæogene aflejringer over Danskekalken. In: Nielsen, O.B. (Ed.), Aarhus Geokompendier No. 1, Danmarks geologi fra Kridt tili dag, 69–114.

Heilmann–Clausen, C., and Schmitz, B., 2000. The late Paleocene maximum $\delta^{13}C$ excursion in Denmark? Geologiska Föreningen i Stockholm Förhandlingar, 122, 70.

Hollis, C. J., Dickens, G. R., Field, B. D., Jones, C. M., and Strong, C. P. 2005. The Paleocene-Eocene transition at Mead Stream, New Zealand: a southern Pacific record of early Cenozoic global change. Palaeogeography, Palaeoclimatology, Palaeoecology 215, 313–343.

Jaramillo, C., Ochoa, D., Contreras, L., Pagani, M., Carvajal-Ortiz, H., Pratt, L.M., Krishnan, S., Cardona, A., Romero, M., Quiroz, L., Rodriguez, G., Rueda, M.J., de la Parra, F., Moran, S., Green, W., Bayona, G., Montes, C., Quintero, O., Ramirez, R., Mora, G., Schouten, S., Bermudez, H., Navarrete, R., Parra, F., Alvaran, M., Osorno, J., Crowley, J.L., Valencia, V., and Vervoort, J., 2010. Effects of rapid global warming at the Paleocene-Eocene boundary on neo tropical vegetation. Science, 330, 957–961.

John, C.M., Banerjee, N.R., Longstaffe, F.J., Sica, C., Law, K.R., and Zachos, J.C., 2012. Clay assemblage and oxygen isotopic constraints on the weathering response to the Paleocene–Eocene thermal maximum, east coast of North America. Geology, 40, 591–594.

John, C.M., Bohaty S.M., Zachos J.C., Sluijs A., Gibbs S., Brinkhuis H., and Bralower T.J., 2008. North American continental margin records of the Paleocene-Eocene thermal maximum: Implications for global carbon and hydrological cycling. Paleoceanography, 23, PA2217.

Kaiho, K., Arinobu, T., Ishiwatari, R., Morgans, H. E. G., Okada, H., Takeda, N., Tazaki, K., Zhou, G., Kajiwara, Y., Matsumoto, R., Hirai, A., Niitsuma, N., and Wada, H., 1996. Latest Paleocene benthic foraminiferal extinction and environmental change at Tawanui, New Zealand. Paleoceanography, 11, 447–465.

Kender, S., Stephenson, M.H., Riding, J.B., Leng, M.J., O'BKnox, R.W., Peck, V.L., Kendrick, C.P., Ellis, M.A., Vane, C.H., and Jamieson, R., 2012. Marine and terrestrial environmental changes in NW Europe preceding carbon release at the Paleocene–Eocene transition. Earth and Planetary Science Letters, 353–354, 108–120.

Knox, R.W.O'B., 1998. In: Aubry, M.-P., Lucas, S.G., and Berggren, W.A.(Eds.),The tectonic and volcanic history of the North Atlantic region during the Paleocene–Eocene transition: implications for NW Europe and global biotic events. Columbia Univ. Press, New York, 91–102.

Kopp, R.E., Schumann, D., Raub, T.D., Powars, D.S., Godfrey, L.V., Swanson-Hysell, N.L., Maloof, A.C., and Vali, H. 2009. An Appalachian Amazon? Magnetofossil evidence for the development of a tropical river-like system in the mid-Atlantic United States during the Paleocene- Eocene thermal maximum. Paleoceanography, 24, PA4211.

Kraus, M.J. and Riggins, S., 2007. Transient drying during the Paleocene–Eocene Thermal Maximum (PETM): analysis of paleosols in the Bighorn Basin, Wyoming. Palaeogeography, Palaeoclimatology, Palaeoecology, 245, 444–461.

Kraus, M.J., McInerney, F.A., Wing, S.L., Secord, R., Baczynski, A.A., and Bloch, J.I., 2013. Paleohydrologic response to continental warming during the Paleocene-Eocene thermal maximum, Bighorn Basin, Wyoming. Palaeogeography, Palaeoclimatology, Palaeoecology, 370, 196–208.

Foreman, B.Z., Heller, P.L., and Clementz, M.T., 2014. Fluvial response to abrupt global warming at the Palaeocene/Eocene boundary. Nature, 491, 92-95.

Gibson, T.G., Bybell, L.M., and Mason, D.B., 2000. Stratigraphic and climatic implications of clay mineral changes around the Paleocene/Eocene boundary of the northeastern US margin. Sedimentary Geology, 134, 65–92.

Lu, G., Adatte, T., Keller, G., and Ortiz, N., 1998. Abrupt climatic, oceanographic and ecological changes near the Paleocene-Eocene transition in the deep Tethys basin: The Alamedilla section, southern Spain. Eclogae Geologicae Helveticae, 91, 293–306.

Nicolo, M.J., Dickens, G.R., and Hollis, C.J., 2010. South Pacific intermediate water oxygen depletion at the onset of the Paleocene-Eocene thermal maximum as depicted in New Zealand margin sections. Paleoceanography, 25, PA4210.

Nicolo, M.J., Dickens, G.R., Hollis, C.J., and Zachos, J.C., 2007. Multiple early Eocene hyperthermals: their sedimentary expression on the New Zealand continental margin and in the deep sea. Geology, 35, 699–702..

Nielsen, O.B., Baumann, J., Zhang, D., Heilmann-Clausen, C., and Larsen, G., 1986. Tertiary deposits in Store Bælt. In: Møller, J.T. (Ed.), Twenty-five Years of Geology in Aarhus, no. 24, Geoskrifter, 235–253.

Pagani, M., Pedentchouk, N., Huber, M., Sluijs, A., Schouten, S., Brinkhuis, H., Sinninghe Damsté, J.S., Dickens, G.R., and the Expedition 302 Scientists, 2006. Arctic hydrology during global warming at the Palaeocene/Eocene Thermal Maximum. Nature 442, 671–675.

Robert, C., and Kennett, J.P., 1994. Antarctic subtropical humid episode at the Paleocene-Eocene boundary: clay mineral evidence. Geology, 22, 211–214.

Schmitz, B. and Pujalte, V., 2003. Sea-level, humidity, and land-erosion records across the initial Eocene thermal maximum from a continental-marine transect in northern Spain. Geology, 31, 689-692.

Schmitz, B. and Pujalte, V., 2007. Abrupt increase in seasonal extreme precipitation at the Paleocene-Eocene boundary. Geology, 35, 215– 218, doi:10.1130/G23261A.1.

Schmitz, B., Pujalte, V., and Nunez-Betelu, K., 2001. Climate and sea-level perturbations during the incipient Eocene thermal maximum: Evidence from siliciclastic units in the Basque Basin (Ermua, Zumaia and Trabakua Pass), northern Spain. Palaeogeography Palaeoclimatology, Palaeoecology, 165, 299 – 320.

Schoon, P.L., Heilmann-Clausen, C., Pagh Schultz, B., Sinninghe Damsté, JS., and Schouten, S., 2015. Warming and environmental changes in the eastern North Sea Basin during the Palaeocene–Eocene Thermal Maximum as revealed by biomarker lipids. Organic Geochemistry, 78, 79–88.

Schulte, P., Scheibner, C., and Speijer, R.P., 2011. Fluvial discharge and sea-level changes controlling black shale deposition during the Paleocene–Eocene Thermal Maximum in the Dababiya Quarry section, Egypt. Chemical Geology, 285, 167-183.

Slotnick, B.S., Dickens, G.R., Nicolo, M.J., Hollis, C.J., Crampton, J.S., Zachos, J.C., and Sluijs, A., 2012. Large-Amplitude Variations in Carbon Cycling and Terrestrial Weathering during the Latest Paleocene and Earliest Eocene: The Record at Mead Stream, New Zealand. The Journal of Geology, 120, 487–505.

Sluijs, A. and Brinkhuis H., 2009. A dynamic climate and ecosystem state during the Paleocene-Eocene thermal maximum: Inferences from dinoflagellate cyst assemblages on the New Jersey Shelf. Biogeosciences, 6, 1755–1781.

Sluijs, A., Bijl, P.K., Schouten, S., Roehl, U., Reichart, G.-J., and Brinkhuis, H., 2011. Southern Ocean warming, sea level and hydrological change during the Paleocene-Eocene thermal maximum. Climate of the Past, 7, 47–61.

Sluijs, A., Bowen, G.J., Brinkhuis, H., Lourens, L.J., and Thomas, E., 2007. The Paleocene-Eocene thermal maximum super greenhouse: Biotic and geochemical signatures, age models and mechanisms of global change. In: Williams M. et al. (eds), Deep-Time Perspectives on Climate Change: Marrying the Signal From Computer Models and Biological Proxies, The Micropalaeontological Society Special Publication, The Geological Society, London, 323–350.

Sluijs, A., Schouten, S., Pagani, M., Woltering, M., Brinkhuis, H., Sinninghe Damsté, J.S., Dickens, G.R., Huber, M., Reichart, G.J., and Stein, R., 2006. Subtropical Arctic Ocean temperatures during the Palaeocene/Eocene Thermal Maximum. Nature 441, 610–613.

Sluijs, A., Brinkhuis, H., Crouch, E.M., John, C.M., Handley, L., Munsterman, D., Bohaty, S.M., Zachos, J.C., Reichart, G.J., Schouten, S., Pancost, R.D., Sinninghe Damsté, J.S.,Welters, N.L.D., Lotter, A.F., and Dickens, G.R., 2008. Eustatic variations during the Paleocene–Eocene greenhouse world. Paleoceanography 23, PA4216.

Stassen, P., Thomas, E., and Speijer, R.P., 2012a. Integrated stratigraphy of the Paleocene–Eocene thermal maximum in the New Jersey Coastal Plain: towards understanding the effects of global warming in a shelf environment. Paleoceanography, 27, PA4210.

Stassen, P., Thomas, E., and Speijer, R.P., 2012b. The progression of environmental changes during the onset of the Paleocene–Eocene thermal maximum (New Jersey Coastal Plain). Austrian Journal of Earth Sciences, 105, 169–178.

Stassen, P., Thomas, E., Speijer, R.P., 2015. Paleocene–Eocene Thermal Maximum environmental change in the New Jersey Coastal Plain: benthic foraminiferal biotic events. Marine Micropaleontology, 115, 1–23.

Storme, J.-Y., Dupuis, C., Schnyder, J., Quesnel, F., Garel, S., Iakovleva, A.I., Iacumin, P., Di Matteo, A., Sebilo, M., and Yans, J., 2012. Cycles of humid-dry climate conditions around the P/E boundary: new stable isotope data from terrestrial organic matter in Vasterival section (NW France). Terra Nova, 24, 114–122.

Tipple, B.J., Pagani, M., Krishnan, S., Dirghangi, S.S., Galeotti, S., Agnini, C., Giusberti, L., and Rio, D., 2011. Coupled high-resolution marine and terrestrial records of carbon and hydrologic cycles variations during the Paleocene-Eocene Thermal Maximum (PETM). Earth and Planetary Science Letters, 311, 82 – 92.

White P.D. and Schiebout J., 2008. Paleogene paleosols and changes in pedogenesis during the initial Eocene thermal maximum: Big Bend National Park, Texas, USA. GSA Bulletin, 120, 1347–1361.

Willumsen, P.S., Schultz, B.P., and Sylvestersen, R., 2014. Rapid Warming at the PETM and its Influence on Vegetation in Denmark. In Rocha R. et al. (eds.), 1st International Congress on Stratigraphy (STRATI 2013), At the Cutting Edge of Stratigraphy, Springer Geology, 159-162.

Wing, S.L., Harrington, G.J., Smith, F.A., Bloch, J.I., Boyer, D.M., and Freeman, K.H., 2005. Transient floral change and rapid global warming at the Paleocene–Eocene boundary. Science 310, 993–996.

Woody, D.T., Smith, J.J., Kraus, M.J., and Hasiotis, S.T., 2014. Manganese-bearing rhizocretions in the Willwood Formation, Wyoming, U.S.A.: implications for paleoclimate during the Paleocene–Eocene thermal maximum. Palaios, 29, 266-276.

Zachos, J.C., Schouten, S., Bohaty, S., Quattlebaum, T., Sluijs, A., Brinkhuis, H., Gibbs, S.J., and Bralower, T.J., 2006. Extreme warming of mid-latitude coastal ocean during the Paleocene–Eocene Thermal Maximum: inferences from TEX86 and isotope data. Geology, 34, 737–740.